Filament Enhancement by Non-linear Volumetric Filtering Using Clustering-Based Connectivity

Ouzounis, Georgios K.; Wilkinson, Michael H.F.

Published in:
ADVANCES IN MACHINE VISION, IMAGE PROCESSING, AND PATTERN ANALYSIS

Publication date:
2006

Citation for published version (APA):
Ouzounis, G. K., & Wilkinson, M. H. F. (2006). Filament Enhancement by Non-linear Volumetric Filtering Using Clustering-Based Connectivity. In N. Zheng, Jiang, & Ian (Eds.), *ADVANCES IN MACHINE VISION, IMAGE PROCESSING, AND PATTERN ANALYSIS* (pp. 317-327). (Lecture Notes in Computer Science; Vol. 4153). Springer.

Filament Enhancement by Non-linear Volumetric Filtering Using Clustering-Based Connectivity

Georgios K. Ouzounis and Michael H.F. Wilkinson

Institute of Mathematics and Computing Science, University of Groningen
P.O. Box 800, 9700 AV Groningen, The Netherlands

Abstract. Shape filters are a family of connected morphological operators that have been used for filament enhancement in biomedical imaging. They interact with connected image regions rather than individual pixels, which can either be removed or retained unmodified. This prevents edge distortion and noise amplification, a property particularly appreciated in filtering and segmentation. In this paper we investigate their performance using a generalized notion of connectivity that is referred to as "clustering-based connectivity". We show that we can capture thin fragmented structures which are filtered out with existing techniques.

1 Introduction

Biomedical data sets often contain curvi-linear, dendritic or other filamentous structures of interest which are susceptible to acquisition noise. Enhancing these structures can be of particular importance to certain medical applications and many methods have been proposed [3]. Some common drawbacks among them is noise amplification and edge distortion while they can also be computationally expensive.

In mathematical morphology, a family of operators called *connected filters* has been developed which interact with regions characterized by some notion of connectivity. According to these filters, *connected regions* can either be removed or retained unmodified based on a pre-specified attribute (shape in this case) but new edges cannot emerge. This edge and therefore shape-preserving property makes connected filters competitive to existing morphological methods for filament enhancement such as the multi-scale approach in [11].

The objects targeted are thin, plate-like (Fig. 1) and elongated structures which are often fragmented at higher gray-levels according to the standard connectivity. We aim at countering this with a further improvement of the method presented in [11]. This is by using a more general notion of connectivity termed *clustering-based connectivity* [8, 9] which models object clusters as individual connected regions. We demonstrate our findings and compare them to the existing method using three different 3-D data sets. In each case we study the parameters which maximize the filter's performance in association with the underlying clustering-based connectivity.

Following this section there is a short reference to the concept of connectivity and connectivity openings complemented by the notion of clustering-based connectivity. In Section 3 the shape filters and their extensions to gray-scale are presented while in Section 4 we discuss their applications to 3-D medical data sets. The work is summarized with some conclusions in Section 5.
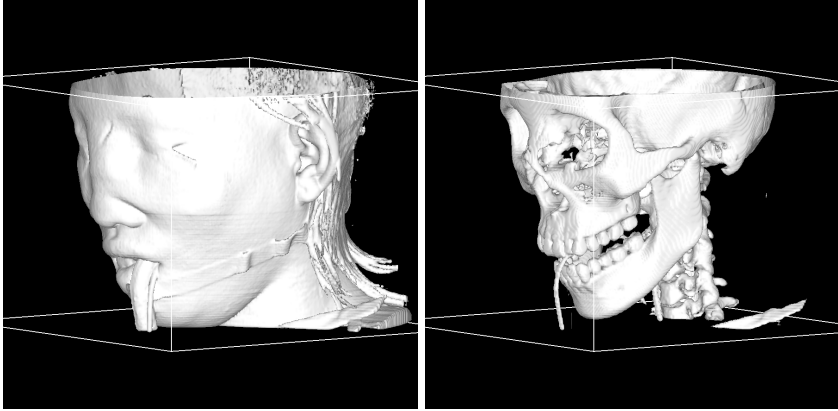
Fig. 1. 3-D Shape filtering using 26 connectivity: The image on the left illustrates an isosurface projection of a human head at isolevel 208. Increasing the isolevel to visualize the skull removes important details. The image on the right illustrates a shape filter enhancing the thin, plate-like structures comprising the skull and all the noise at an isolevel 96.

2   Theory

2.1   Connectivity Classes and Openings

The set-theoretic notion of connectivity in discrete spaces such as $\mathbb{Z}^2$ describes how groupings are realized in digital images. Connectivity in mathematical morphology is given by *connectivity classes*, a construct defined as:

Definition 1. *Let E be an arbitrary (non-empty) set. A family $\mathcal{C} \subseteq \mathcal{P}(E)$ is called a* connectivity class *if it satisfies:*

1. *$\emptyset \in \mathcal{C}$ and for all $x \in E$, $\{x\} \in \mathcal{C}$,*
2. *for any $\{A_i\} \subseteq \mathcal{C}$ for which $\bigcap A_i \neq \emptyset \Rightarrow \bigcup A_i \in \mathcal{C}$*

Members of $\mathcal{C}$ are called *connected sets* [8, 9] and Definition 1 means that both the empty set and singleton sets are connected, and any union of connected sets which have a non-empty intersection is also connected.

Addressing objects in binary images is often more practical using *connected components* or *grains* which are connected parts of an object of maximal extend, i.e. they are connected and not smaller than any other connected part of the same object. Writing this explicitly, we say that C is a connected component of a binary image X if there is no set $C' \supset C$ such that $C' \subseteq X$ and $C' \in \mathcal{C}$.

Connected components are groupings of connected sets containing a certain point $x \in E$ in their intersection. The operator Γ_x to access them is called a *connectivity opening* marked by x and is given by:

$$\Gamma_x(X) = \bigcup \{A_i \in \mathcal{C} \mid x \in A_i \text{ and } A_i \subseteq X\}. \tag{1}$$

Furthermore, $\forall x \notin X$, $\Gamma_x(X) = \emptyset$. Connectivity openings are characterized by three properties; they are *anti-extensive*, *increasing* and *idempotent* operators. For a given set X each property implies the following:

1. Anti-extensiveness: $\Gamma_x(X) \subseteq X$,
2. Increasingness: if $X \subseteq Y \Rightarrow \Gamma_x(X) \subseteq \Gamma_x(Y)$,
3. Idempotence : $\Gamma_x(\Gamma_x(X)) = \Gamma_x(X)$.

The operator Γ_x is explicitly related to a connectivity class $\mathcal{C}$ if satisfying the set of conditions given by Serra [8] (also in [6]) in the following theorem:

Theorem 1. *The datum of a connectivity class $\mathcal{C}$ on $\mathcal{P}(E)$ is equivalent to the family $\{\Gamma_x \mid x \in E\}$ of openings on x such that:*

1. *every Γ_x is an algebraic opening,*
2. *for all $x \in E$, we have $\Gamma_x(X) = \{x\}$,*
3. *for all $X \subseteq E$, $x, y \in E$, $\Gamma_x(X)$ and $\Gamma_y(X)$ are equal or disjoint,*
4. *for all $X \subseteq E$, and all $x \in E$, we have $x \notin X \Rightarrow \Gamma_x(X) = \emptyset$.*

Connectivity openings characterize uniquely the connectivity class they are associated with and there is a one-to-one correspondence between the two.

2.2   Clustering-Based Connectivity

Connected components of X according to $\mathcal{C}$ are separated by elements of the background. If however the distance separating them is smaller than the size of a given structuring element (SE), it is possible to define a *cluster* [1,6,9] in a *child* connectivity class $\mathcal{C}^\psi$, where ψ denotes a structural operator referred to as *clustering*. Following is a list summarizing the properties required to define a clustering:

1. ψ is increasing and extensive.
2. $\psi(\mathcal{C}) \subseteq \mathcal{C}$.
3. For a family $\{X_i\}$ in $\mathcal{P}(E)$ such that $\psi(X_i) \in \mathcal{C}$, $\forall~i$, and $\bigcap_i X_i \neq \emptyset \Rightarrow \psi(\bigcup X_i) \in \mathcal{C}$.
4. ψ does not create connected components; i.e., if $\forall x \in C$, $C = \Gamma_x(\psi(X)) \Rightarrow X \cap C \neq \emptyset$.
5. ψ treats the clusters of X independently; i.e., if $\forall x \in C$, $C = \Gamma_x(\psi(X)) \Rightarrow \psi(X \cap C) = C$.

More details on each item are given in [1]. Typically, ψ is either a dilation or a closing and generates a mask image, called the *connectivity mask* by expanding X.

Definition 2. *Let $\mathcal{C}$ be a connectivity class in $\mathcal{P}(E)$ and ψ be an increasing and extensive operator on $\mathcal{P}(E)$. Then*

$$\mathcal{C}^\psi = \{X \in \mathcal{P}(E) \mid \psi(X) \in \mathcal{C}\} \tag{2}$$

is a clustering-based *connectivity class for which $\mathcal{C} \subseteq \mathcal{C}^\psi$.*

If, for ψ the above five properties hold, and furthermore, $\psi(\emptyset) = \emptyset$ and

$$\psi(X \cap \Gamma_x(\psi(X))) = \Gamma_x(\psi(X)), \tag{3}$$

we have a *strong clustering* [1].

Definition 3. *Let $\{\Gamma_x \mid x \in E\}$ be the connectivity openings associated with $\mathcal{C}$. If ψ is a strong clustering on $\mathcal{P}(E)$, the family of connectivity openings $\{\Gamma_x^\psi \mid x \in E\}$ associated to $\mathcal{C}^\psi$ are given by*

$$\Gamma_x^\psi(X) = \begin{cases} \Gamma_x(\psi(X)) \cap X, & \text{if } x \in X \tag{4a} \\ \emptyset, & \text{otherwise} \tag{4b} \end{cases}$$

In the following, every time we use the term clustering we mean a strong clustering.

3   Shape Filters

Filtering a binary image based on the attributes of its connected components requires a criterion T commonly given by:

$$T(C) = (Attr(C) \geq \lambda) \tag{5}$$

where $Attr$ is some attribute value of a connected component C and λ a pre-selected threshold. Components that satisfy (5) are retained while the rest are removed. Binary attribute filters in the anti-extensive case can be categorized to attribute openings or thinnings depending on whether the attribute criterion is increasing or not. The case that $Attr(C)$ is non-increasing implies that for any two nested components C_1 and C_2,

$$C_1 \subseteq C_2 \nRightarrow Attr(C_1) \leq Attr(C_2), \tag{6}$$

i.e. their attributes need not be ordered in the same way. Comparing the attribute value of a connected component against λ is by means of a trivial thinning Φ_T on the output of the connectivity opening of (1). The trivial thinning is an anti-extensive, idempotent and non-increasing operator defined as $\Phi_T : \mathcal{C} \to \mathcal{C}$ which for a connected component $C \in \mathcal{C}$ yields C if $T(C)$ is true, and $\emptyset$ otherwise. Furthermore, $\Phi_T(\emptyset) = \emptyset$. For a binary image X, the attribute thinning is given by:

$$\Phi^T(X) = \bigcup_{x \in E} \Phi_T(\Gamma_x(X)). \tag{7}$$

Attribute thinnings sensitive to structures of a given shape are called *shape filters*. The filamentous structures that we investigate, are thin elongated structures that are characterized by a high trace of the moment of inertia tensor $I(C)$ compared to their volume $V(C)$. For 3-D data sets, $I(C)$ has a minimum for a sphere and increases rapidly as the object becomes more elongated [11]. It is defined as:

$$I(C) = \frac{V(C)}{4} + \sum_{\mathbf{x} \in \mathbf{C}} (\mathbf{x} - \overline{\mathbf{x}})^{\mathbf{2}} \tag{8}$$

and scales with size to the fifth power whereas the volume scales with the third power of the size. Therefore the ratio

$$Attr(C) = \frac{I(C)}{V^{5/3}(C)} \tag{9}$$

is a purely shape dependent attribute which together with (7) defines a filter sensitive to elongated shapes.

Connected filters in general rely on some notion of connectivity. In the case of (7) the term $\Gamma_x(X)$ relates the filter to the connectivity class $\mathcal{C}$ and the connected components it returns are unique. Extending connected filters to sets characterized by second-generation connectivity is by replacing the connectivity opening with the associated operator. For clustering-based connectivity this is Γ_x^{ψ}.

The cases in which the attribute criterion of a filter is increasing, like the volume of a 3-D connected component $V(C)$, extend to gray-scale trivially [4, 5] based on the principle of threshold superposition [2]. For the non-increasing, translation and shift invariant shape descriptor of (9), gray-scale attribute filters based on either type of connectivity can be computed efficiently using the *subtractive filtering rule* [10]. This is a non-pruning, tree-based filtering strategy in which if a tree node (corresponding to a connected component of the thresholded image at level h) is reduced in gray-scale, its descendants are lower by the same amount. It is realized on a tree structure for second-generation connectivity representation termed the *Dual-Input Max-Tree* algorithm that is based on [7] and extended details can be found in [4, 5]. The experiments that follow are based on this arrangement.

4   Experiments

In this section we experiment with the 3-D shape filter discussed in Section 3, using clustering-based connectivity. In this first approach to non-linear volumetric filtering using this specific type of second-generation connectivity, the objective is to enhance and extract filamentous details from a number of noisy biomedical data sets. The present study investigates the factors that affect the performance of the proposed filter. We identify five critical parameters namely: (i) the neighborhood of each volume element in 3-D, (ii) the size of the structuring element to be used, (iii) the type of clustering operator ψ, i.e. a dilation or a closing, (iv) the way the attributes are calculated (on X or $\psi(X)$) and (v) the attribute threshold used with the filter.

The first data set is an isosurface projection of an 8 bit, $256 \times 256 \times 256$ rotational b-plane CT-angiogram (CTA) of the arteries of the right half of a human head (Fig. 2). A contrast agent was used and an aneurysm is present. The volume contains a dense cloud of low intensity noise centered within the structures of interest. To generate the connectivity mask we consider the first three parameters listed earlier. For volume sets it is common to use a 26 neighborhood since a 6 neighborhood often results in "loosely" connected components. Masks generated by a dilation expand the original set creating a number of structures of previously disconnected elements. In noisy backgrounds, this can result in grouping the noise elements to high attribute structures and create connections with the structures of interest. Using structural closings instead, the unwanted
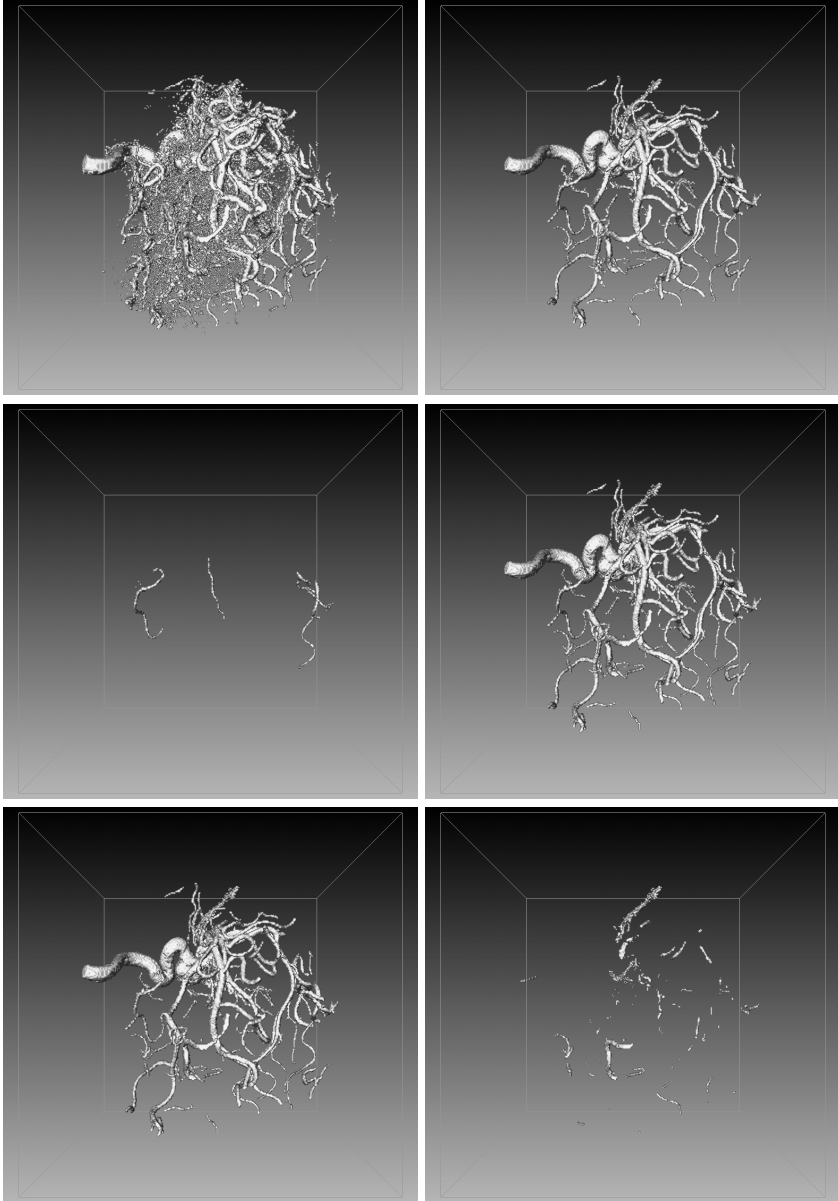
Fig. 2. Isosurface projections of a CTA scan containing an aneurysm and the output of the elongation filter based on standard connectivity (both at isolevel 0). The middle row shows the filtered outputs using a mask based on a dilation and a closing respectively. The bottom row shows the difference volumes between the filter outputs using clustering-based connectivity based on a closing vs. a dilation and based on a closing vs. the standard connectivity. Most vessel-like structures are preserved using a closing-based connectivity.

connections between small objects tend to break apart while structures merged by wide bridging regions are maintained. This is illustrated at the middle row of Fig. 2 where the image on the left shows the response of an elongation filter with $\lambda=3$ using a mask based on a dilation with a cubic SE of size $3 \times 3 \times 3$. The image on the right is the response of the same filter using a mask by a structural closing instead. It is evident that a dilation even with a relatively small SE merges most of the noise together with the blood vessels creating a structure with large overall volume and small elongation. Filtering removes all but certain regions disconnected from the clustered volume. The results can be compared with the filter response using standard, 26-connectivity - top right image. The bottom row shows the difference volumes between the filter responses. In the left image we compare the responses using a closing and a dilation. It can be seen that most of the structure of interested is lost. The right image shows the difference in the response using a closing-based clustering connectivity and the standard connectivity. We see a number of elongated structures missed by the filter using standard connectivity. With the closing-based connectivity, these vessel fragments are merged with the overall structure and hence they are retained.

The second data set shown at the top left image of Fig. 3, is a $256 \times 342 \times 243$, 8-bit confocal microscopy volume of a pyramidal neuron. The noise density here is not as high as the previous data set, but the filamentous structures (the dendrites in this case) are fragmented at low levels. Filtering using standard connectivity removes noise together with a considerable fraction of the dendrites. If the volume is clustered however, nearby fragments are connected into a single entity with overall elongation greater than the threshold λ and hence are retained. The top right image shows the result of an elongation filter with $\lambda=2$ using the standard connectivity at a 26 neighborhood.

Creating a mask with a structural closing is often not sufficient to counter the issue of noise clustering. Noise can be clustered in arbitrary arrangements and along arbitrary orientations. Two examples are illustrated at the first two images of Fig. 4 where both clustered arrangements have a similar elongation measure (attributes computed on the clustered sets are referred to as *C-attributes*). If the elongation measure is computed based on the expanded sets as illustrated at the corresponding connectivity masks at the last two images, the attributes of the two clustered arrangements are separated by a larger margin that distinguishes easier compact from elongated clusters. Attributes computed on the expanded sets of the mask are referred to as *M-attributes*.

The two images of the middle row of Fig. 3 illustrate the filter response with a connectivity mask generated by a structural closing with a cubic SE of size $5 \times 5 \times 5$ and corresponding C- and M-attributes respectively. The difference volumes computed between the responses with C-attributes, and M-attributes vs. 26-connected filtering, respectively, are shown at the bottom row. It can be seen that together with a considerable fraction of the dendrites claimed by the filter based on clustering connectivity, computing M-attributes outperforms the output based C-attributes which fails to deal with clustered noise effectively. The top first four images are isosurface projections at level 1 and the last two at level 0.

The last data set is a $256 \times 256 \times 124$, 8-bit, phase contrast magnetic resonance angiogram (MRA) of a human head. In this experiment we target the blood vessels and experiment with the size of the SE to be used along ψ in generating the connectivity
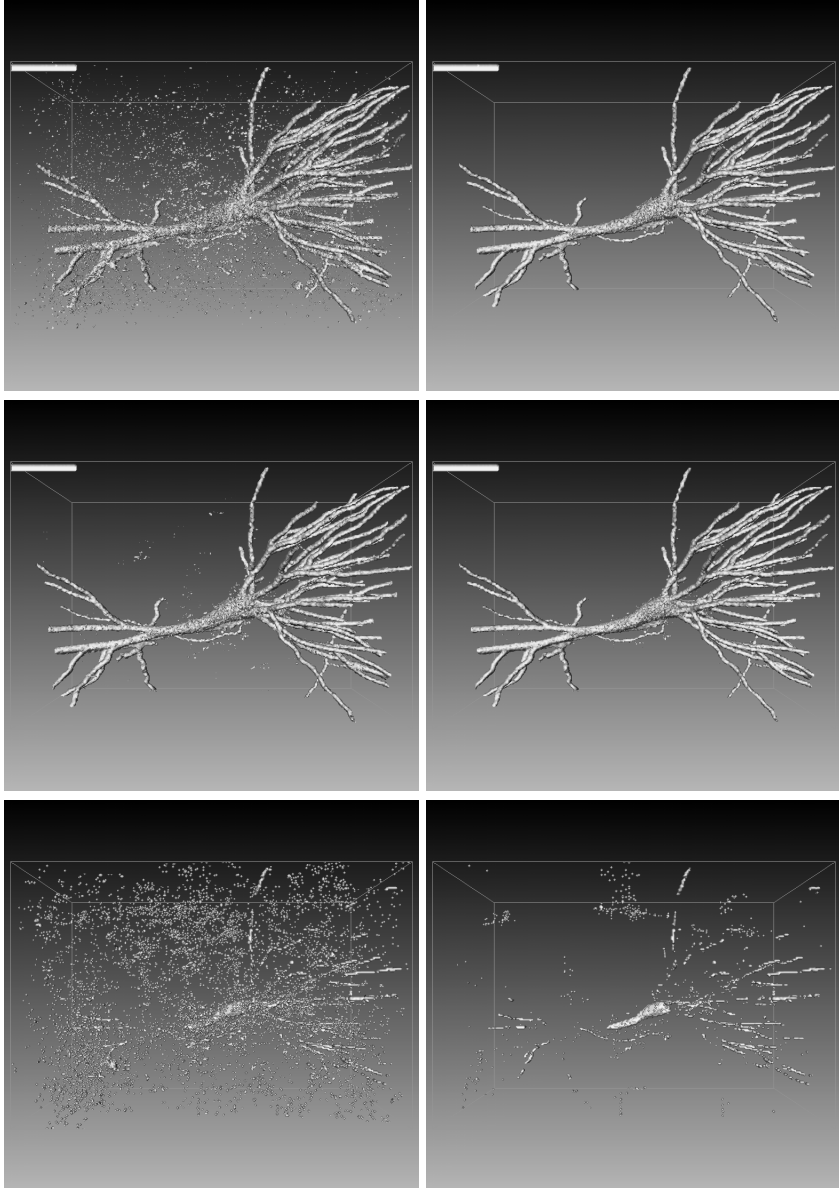
Fig. 3. Isosurface projections of the neuron and the output of the elongation filter based on the standard connectivity, both at isolevel 1. The middle row illustrates the filter performance by computing the structure attributes based on the clustered volume and based on the expanded volume which constitutes the mask. The bottom row shows the difference volumes between the C-attributes vs. 26-connected filtering, and between the M-attributes vs. 26-connected filtering.

Fig. 4. The elongation measures of the clustered sets X and Y (first and second image from the left) are similar if the we compute the C-attributes. The M-attributes instead are computed on $\psi(X)$ and $\psi(Y)$ (third and fourth image from the left respectively) and obviously the elongation of $\psi(X)$ is smaller compared to that of $\psi(Y)$.

mask. The top left image of Fig. 5 shows the input volume at isolevel 50 (details start to appear only after this threshold). The top right image and the two at the middle row (starting from the left) show the responses of an elongation filter with $\lambda = 2$ using standard connectivity, and clustering connectivity based on masks by a $3 \times 3 \times 3$ and $5 \times 5 \times 5$ cubic SE respectively (at isolevel 5). The filter uses M-attributes and from the difference volumes between the responses of the filter using clustering connectivity with 3^3-based mask vs. standard connectivity and with 5^3-based mask vs. standard connectivity, it can be seen that both deal relatively well with clustered noise (isolevel 1) and they both capture vessel fragments but at a varying detail. To examine their in-between differences we also compute the difference volume between the output with 3^3-based mask vs. 5^3-based mask and the reverse (Fig. 6). The left image illustrates that with an increasing size of SE, the overall signal intensity in the vessels is reduced, though there is no distortion. On the other hand as the size of the SE increases the number of fragments captured increases as well, as shown in the righthand image. This also contributes to some additional clustered noise. In general the size of the SE can only be determined by the amount of detail required and a quantitative evaluation is only possible given the ground truth.

5   Discussion

In this paper we compared the performance of connected filters for filament enhance-ment, based on classical connectivity and clustering-based connectivity. From the dif-ference volumes produced in the previous section it can be seen that the 3-D shape filter, sensitive to elongated structures, captures filamentous details in greater accuracy when dependent upon an underlying clustering-based connectivity. This is because fragments of the filamentous structures are clustered with their original body, contributing to an overall elongation attribute greater than their own if treated separately.

The parameters influencing the performance of the filter have also been studied and we demonstrated how each one affects the filter response and in what way. A compari-son with different elongation thresholds has not been carried out since it is obvious that as the value of λ increases the more elements will be filtered out. This can be useful for capturing highly elongated structures. In the case of blood vessels the handling of each vessel separately involves a different type of second-generation connectivity called *contraction-based connectivity* which is not studied here.

A drawback of filters relying on a clustering-based connectivity is that of noise clus-tering. We minimize this effect by considering the structure attributes based on the
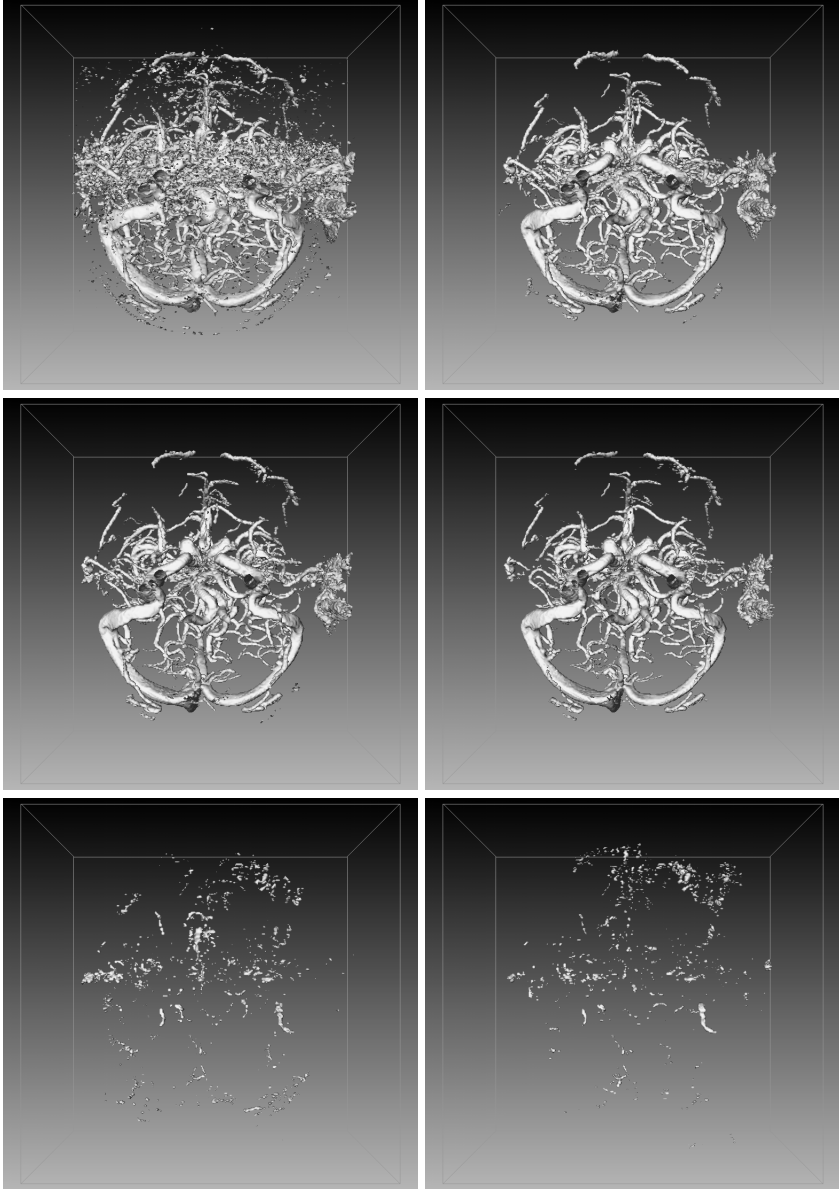
Fig. 5. Isosurface projection of the MRA at isolevel 50 and the output of the elongation filter based on the standard connectivity at isolevel 5. The middle row illustrates the filter outputs using a clustering-based connectivity with masks generated by a structural closing with a cubic SE of size $3 \times 3 \times 3$ and $5 \times 5 \times 5$ respectively. The bottom row shows the difference volumes between the two filter outputs compared against the volume generated by the filter based on standard connectivity.
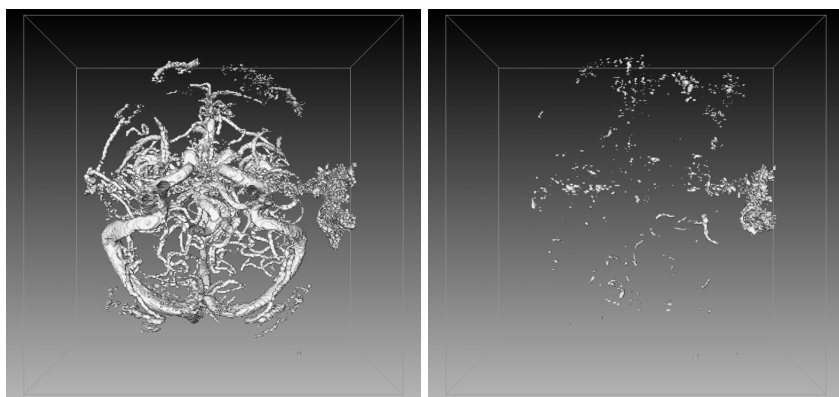
Fig. 6. The difference volumes between a filter based on the 3^3-based mask vs. the 5^3-based mask, and the reverse, at isolevel 1

connectivity mask instead of the clustered volume. We are currently working on further improvements by creating connectivity masks with adaptive structuring elements sensitive only to the direction of elongation.

References

1. U.M. Braga-Neto and J. Goutsias. Connectivity on complete lattices: New results. *Comp. Vis. Image Understand.*, 85:22–53, 2002.
2. P. Maragos and R. D. Ziff. Threshold superposition in morphological image analysis systems. *IEEE Trans. Pattern Anal. Mach. Intell.*, 12(5):498–504, 1990.
3. M. Orkisz, M. Hernández-Hoyos, P. Douek, and I. Magnin. Advances of blood vessel morphology analysis in 3D magnetic resonance images. *Mach. Vis. Graph.*, 9:463–471, 2000.
4. G. K. Ouzounis and M. H. F. Wilkinson. Mask-based second-generation connectivity and attribute filters. *IEEE Trans. Pattern Anal. Mach. Intell.*, 2005. submitted.
5. G. K. Ouzounis and M. H. F. Wilkinson. Second-order connected attribute filters using maxtrees. In C. Ronse, L. Najman, and E. Decencire, editors, *Mathematical Morphology: 40 Years On; Proc. 7th Int. Symp. Math. Morphology*, pages 65–74. Springer-Verlag, 2005.
6. C. Ronse. Set-theoretical algebraic approaches to connectivity in continuous or digital spaces. *Journal of Mathematical Imaging and Vision*, 8:41–58, 1998.
7. P. Salembier, A. Oliveras, and L. Garrido. Anti-extensive connected operators for image and sequence processing. *IEEE Trans. Image Proc.*, 7:555–570, 1998.
8. J. Serra, editor. *Image Analysis and Mathematical Morphology. II: Theoretical Advances*. Academic Press, London, 1988.
9. J. Serra. Connectivity on complete lattices. *Journal of Mathematical Imaging and Vision*, 9:231–251, 1998.
10. E. R. Urbach and M. H. F. Wilkinson. Shape-only granulometries and grey-scale shape filters. In H. Talbot and R. Beare, editors, *Mathematical Morphology; Proc. 6th Int. Symp. Math. Morphology*, pages 305–314, Collingwood, Australia, 2002. CSIRO Publishing.
11. M. H. F. Wilkinson and M. A. Westenberg. Shape preserving filament enhancement filtering. In W. J. Niessen and M. A. Viergever, editors, *Proc. MICCAI'2001*, volume 2208 of *Lecture Notes in Computer Science*, pages 770–777, 2001.